Prediction of corrosion behavior using neural network as a data mining tool

Mst Kamrunnahar *, Mirna Urquidi-Macdonald

Department of Engineering Science and Mechanics, The Pennsylvania State University, 212 EES Building, University Park, PA 16802, USA

ABSTRACT

A supervised neural network (NN) method was used as a data mining tool to predict corrosion behavior of metal alloys. The NN model learned the underlying laws that map the alloy's composition and environment to the corrosion rate. Existing corrosion data on corrosion allowable as well as corrosion resistive alloys were collected for both DC and AC corrosion experiments. The data mining results allow us to categorize and prioritize certain parameters (i.e. pH, temperature, time of exposure, electrolyte composition, metal composition, etc.) and help us understand the synergetic effects of the parameters and variables on electrochemical potentials and corrosion rates.

© 2009 Elsevier Ltd. All rights reserved.

1. Introduction

'Data mining' can be defined as "extraction of knowledge and information from large amount of data", or other information repositories. Data mining has applications in a wide range of subjects, including science and technology. The goal of data mining varies according to the application. There are a number of steps involved in data mining, such as: (i) data collection and formatting, (ii) data cleaning, (iii) data integration, (iv) data transformation, (v) data mining or knowledge extraction, (vi) pattern evaluation, and (vii) knowledge presentation [1]. The first four items can be termed together as the "pre-processing" step in data mining and are done in a way that the 'pre-processed' data can be used in the later steps for specific applications. The fourth and fifth items fall into the "analysis" step in data mining and follow the goal as to what knowledge the user is looking for and the last step is how to present the findings of the mining process. 'Analysis' in data mining can be divided into two categories: (1) directed data mining that includes classification, estimation, and prediction and (2) undirected data mining that includes affinity grouping or association rules and clustering [2]. In this paper, we focus on prediction data mining and the system of our interest is the corrosion behavior of metals and alloys.

Although corrosion behavior has been studied for decades, if not centuries, one of the most important scientific challenges in corrosion studies of certain metals and alloys is to learn the trends that govern the long term corrosion behavior. Sometimes environmental effects on alloy behavior are not well understood and most of

the parameters that play a role on the alloy's potential response are difficult to directly or indirectly measure or quantify. This is particularly correct if the alloys are good corrosion resistant in a given environment and it takes considerable time for them to reach steady state. Because the experimental work domain includes parameters hard to quantify and evaluate, producing data and fitting polynomials to that data in order to extrapolate alloy behaviors over extended period may not be suitable. Data mining, applying to corrosion, represents an assortment of tools available to quantify the response that a given alloy sample will have under a given imposed environment and the effect that the environmental changes have on the alloy sample. These tools require well controlled experimentation in well chemically defined environments. Corrosion data on metal alloys are commonly used to obtain unknown parameters in the deterministic theoretical models; in order to accurately portray the laws that govern the alloy's behavior under any environmental condition (generally). Then those models, once those parameters are obtained from data fitting, are used to make "long term" corrosion predictions and prediction on a wider range of environments for the alloy under study. This scientific exercise to create a model and fit measured data to obtain unknown parameters is necessary to develop a predictive methodology that spare us from carrying out infinite measurements – if the metal alloy under study is very good corrosion resistant. Data mining "short-cuts" the deterministic model and provides a "hidden" map between measured alloy characteristics, environments, and the experimental failure observations on the alloy under research. In the data mining we carried out, special emphasis was given to categorizing the importance of the role of different parameters on the corrosion rates. The results of the data mining approach were compared and contrasted to some of the

---

* Corresponding author. Tel.: +1 814 865 0663; fax: +1 814 865 6161.
E-mail address: muk11@psu.edu (M. Kamrunnahar).

experimental data available. The map established was used to extrapolate the alloys' corrosion and crevice potentials and crevice or crack grow rates over much longer times as a function of the changing environment.

In our analysis, corrosion potential data (polarization curves) on metallic glasses [3], corrosion rate and weight loss data on carbon and alloy steel [4,5], and crevice corrosion data on grade-2 titanium [6] were used for comparison and future prediction of the alloys' corrosion behavior. These alloys were chosen mainly because of the availability of data and were used to investigate the efficacy of the data mining tools for corrosion estimation and prediction. These tools can well be applied to the corrosion prediction of other metals and alloys.

In this paper, we give a brief introduction on artificial neural network in Section 2. We describe the data collected on metal alloys for general and localized corrosion in Section 3. Database mining of general corrosion data using neural network is discussed in Section 4. Database analysis and results obtained form data mining of localized corrosion data are presented in Section 5. Summary on the data analysis is presented in Section 6 of this paper.

2. Neural network backpropagation method

An artificial neural network (ANN) is a computational model based on biological neural networks and consists of an interconnected group of artificial neurons [7–10]. Fig. 1(a) shows a simple example of an ANN. It can be treated as non-linear statistical data modeling tools that can be used to model complex relationships between inputs and outputs or to find patterns in data. Advantages of an ANN include: (i) an ANN can perform tasks that a linear program cannot, (ii) when an element of the neural network fails, it can continue without any problem by their parallel nature, (iii) a neural network learns and does not need to be reprogrammed, and (iv) it can be implemented in any application without any problem. However, the disadvantages of an ANN include: (i) an ANN needs training to operate and (ii) requires high processing time for large neural networks.

There are mainly two learning processes of an ANN namely supervised learning and unsupervised learning. In supervised learning, for a given a set of input–output pairs, the aim is to find a function that maps the inputs to the outputs by minimizing a cost function that is related to the mismatch between the mapped outputs and the target outputs. A commonly used objective is to minimize the average squared error between the network's outputs and the target values. When one tries to minimize this mean-squared error cost function using a gradient descent algorithm for a class of neural networks called Multi-Layer Perceptrons, one obtains the well-known backpropagation algorithm for training neural networks. Fig. 1(b) shows an example of an extended network to estimate the cost function. Let us consider a given training set $\{(x_1, t_1), \ldots, (x_p, t_p)\}$ consisting of p ordered pairs of n- and m-dimensional vectors, which are called the input and output patterns. The weights of the edges are real numbers selected at random. When the input pattern x_i from the training set is presented to this network, it produces an output o_i different in general from the target t_i. Typically, the objective is to make o_i and t_i identical for $i = 1, \ldots, p$, by using a learning algorithm. More precisely, the objective is to minimize the error function of the network, defined as

$$E = \frac{1}{2} \sum_{i=1}^{p} \|o_i - t_i\|^2 \tag{1}$$

For more information on NN backpropagation method, see Chapter 7 of Ref. [11].

3. Data collection on general and localized corrosion of metal alloys

We have collected corrosion related data on metal alloys with different corrosion behavior. Data presented in this paper were collected from mainly two sources: (i) publicly available (publications, etc.) and (ii) personal communication. Collected data were divided into (a) general corrosion data and (b) localized corrosion categories. For the analysis, we have selected the following sources:

1. General corrosion:
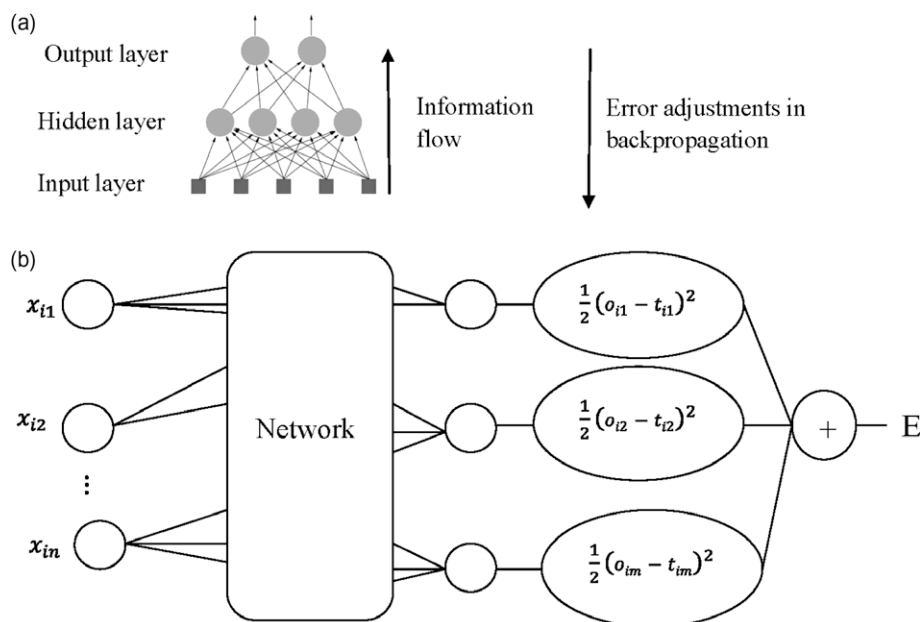   (a)   DC data on metallic glasses, received from publicly available articles [3].

Fig. 1. (a) A simple example of an artificial neural network, (b) an example of an extended network to estimate the cost functions in NN backpropagation.

(b) Corrosion rate data (DC) on carbon and alloy steel from the National Institute of Standards and Technology (NIST) [4,5], received through personal communication.

2. Localized corrosion:
   (a) DC data on grade-2 titanium, received from publicly available articles [6].

We summarize in the following sections a sample of the data we have collected and used for our analysis in this work. The data presented in the tables and graphs are only examples of data collected and not an exhaustive list of all the collected data. Data from multiple experiments, figures, and tables that represent the same corrosion variables were integrated into a single database for further analysis.

4. Database mining of general corrosion data on metal alloys

4.1. General corrosion DC data on iron-alloy ($Fe_{68}Ni_{14-x}Mo_xSi_2B_{16}$ metallic glasses for different x values) using polarization curves [3]

Corrosion potential is a simple measure of corrosion behavior of metals and alloys in the way that the changes in the corrosion potential give an indication of the active or passive behavior of the metal/alloy in hand. Moreover, corrosion potential indicates the thermodynamic corrosion risk of the metal alloy system when viewed in the context of the Pourbaix diagram. Therefore, prediction of corrosion potential and its evolution is important to understand the long term corrosion behavior of metal alloys.

Polarization resistance of a material is defined as the slope of the potential-current density ($dE/d(i)$) curve at the free corrosion potential. Polarization resistance, R_p can be related to the corrosion current by the Stern–Geary equation:

$$R_p = \frac{(\Delta E)}{(\Delta i)_{\Delta E \to 0}}$$

$$\text{Corrosion Rate(mpy)} = 1.287 \times 10^5 \times (\text{eqw}/d) \times I_{corr} \tag{2}$$

$$I_{corr} = \beta_a \beta_c / [2.3 R_p (\beta_a + \beta_c)]$$

where R_p is the polarization resistance, eqw is the equivalent weight of the sample in g mol^{-1}, d is the density in g cm^{-3}, and I_{corr} is the corrosion current density in A/cm^3. β_a and β_c are the Tafel slopes of the anodic and cathodic branches of the polarization curves in Volt per decade, which are associated with transfer coefficients of each reaction.

Glassy alloys are well known for their magnetic properties as well as for other promising properties such as high yield strength, fracture resistance, hardness, and corrosion resistance [12,13]. There have been several studies on the corrosion properties of metallic glasses. A few among them are described in Refs. [14–21].

We here collected DC corrosion data on $Fe_{68}Ni_{14-x}Mo_xSi_2B_{16}$ for several values of x. Figs. 2 and 3 are an example of DC data collected as the polarization curves and Tables 1 and 2 show the type of parameters that can be extracted from these polarization curves. The experimental work to collect the data shown is lengthy and costly. Accordingly, only a limited number of options can be explored. In our tasks, we learnt to "mimic" the polarization curves collected and then calculated corrosion potentials and polarization resistances (R_p).

Neural network (NN) backpropagation method, a supervised learning technique in ANN, was used to fit a model to the collected experimental data (potential and current density) using Neural-Ware Software [22]. The model inputs contained polarization data for $Fe_{68}Ni_{14-x}Mo_xSi_2B_{16}$ metallic glasses with x = 0, 1, 2 in 1 M HCl and x = 0, 1, 2, 3 in 0.5 M H_2SO_4. The topology of the ANN was as follows: 7 inputs, three hidden layers consisting of 100, 100, and
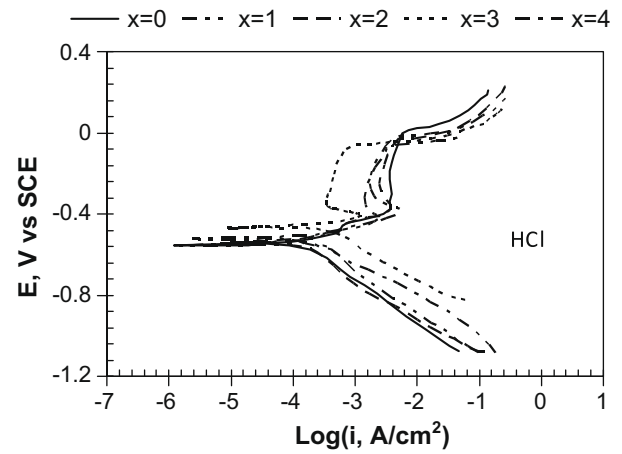

Fig. 2. Polarization curves for $Fe_{68}Ni_{14-x}Mo_xSi_2B_{16}$ metallic glasses with x = 0, 1, 2, 3, 4 in 1 M HCl [3].

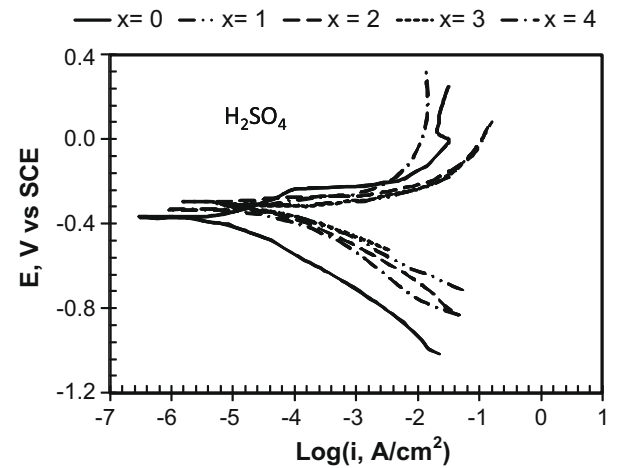**Fig. 3.** Polarization curves for $Fe_{68}Ni_{14-x}Mo_xSi_2B_{16}$ metallic glasses with x = 0, 1, 2, 3, 4 in 0.5 M H_2SO_4 [3].

Table 1
Kinetic parameters from experimental polarization data for $Fe_{68}Ni_{14-x}Mo_xSi_2B_{16}$ metallic glasses with x = 0, 1, 2, 3, 4 in 1 M HCl [3]. β_a and β_c are Tafel constants and R_p is polarization resistance.

Sample	E_{corr}, mV vs SCE	i_{corr}, μA/cm^2	β_a, mV/decade	β_c, mV/decade	R_p, ohm cm^2
x = 0	−57	153	109	203	201
x = 1	−540	226	71	223	103
x = 2	−567	153	79	237	167
x = 3	−506	271	31	154	41
x = 4	−554	141	70	134	142

Table 2
Kinetic parameters from experimental polarization data for $Fe_{68}Ni_{14-x}Mo_xSi_2B_{16}$ metallic glasses with x = 0, 1, 2, 3, 4 in 0.5 M H_2SO_4 [3].

Sample	E_{corr}, mV vs SCE	i_{corr}, μA/cm^2	β_a, mV/decade	β_c, mV/decade	R_p, ohm cm^2
x = 0	−357	13	125	176	2774
x = 1	−290	50	25	103	154
x = 2	−310	400	137	137	148
x = 3	−317	200	169	169	264
x = 4	−331	125	109	109	116

50 neurons, respectively, and 4 outputs. The inputs were: Mo content x, Ni content $(14 - x)$, $(x + 1)$, HCl, H_2SO_4, potential (E), and dE. The outputs were: $\log(i)$, corrosion potential E_{corr}, corrosion current i_{corr}, and polarization resistance R_p. A hyperbolic tangent (tanh) function was used as the transfer function in the ANN model. The Levenberg–Marquardt algorithm was used as the optimization algorithm and the error minimization tolerance was set to 1%. There were 300 samples for training the NN model. Once the NN backpropagation output was "thought" to "mimic" the experimental results, the NN was said to have learned the mapping function between the inputs and the output. The process of learning was obtained by adapting the weights or connections between the neurons contained in the different layers used to design the neural net. Then, the NN backpropagation was ready to be tested. In the testing mode, the weights or neuron connections were not changed and for each input vector, the net reproduced an output. Prediction

of, current density using the potential data as the input was validated using test data sets for $x = 3$, 4 in 1 M HCl and $x = 3$, 4 in 0.5 M H_2SO_4. Note that the test data sets consisting of 141 samples for $x = 3$, 4 in 1 M HCl and $x = 4$ in 0.5 M H_2SO_4 were never used during the training of the NN model.

Results on model validation and prediction in Figs. 4 and 5(a)–(d) show good model-experiment agreement. In Fig. 4(a)–(d), the developed model was validated using the same data sets as were used for the training. These results show if the model was able to capture the system dynamics in, at least, the training data sets. In Fig. 5(a)–(d), the model prediction using new sets of data that were not seen by the model during the training were used. This shows that the model was capable of capturing the system dynamics when the prediction was compared to experimental data. Although slight deviation of the predicted results from the experimental data is observed in Fig. 5(a) and (d), the overall prediction is
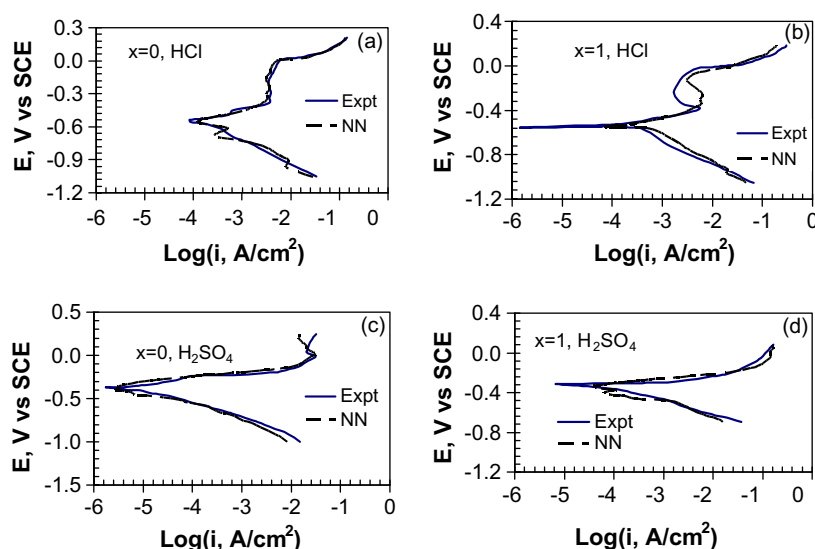

Fig. 4. Experimental and NN predicted polarization curves for $Fe_{68}Ni_{14-x}Mo_xSi_2B_{16}$ metallic glasses with (a) $x = 0$ in 1 M HCl, (b) $x = 1$ in 1 M HCl, (c) $x = 0$ in 0.5 M H_2SO_4, and (d) $x = 1$ in 0.5 M H_2SO_4. The NN prediction used the same data sets that the model was trained with.
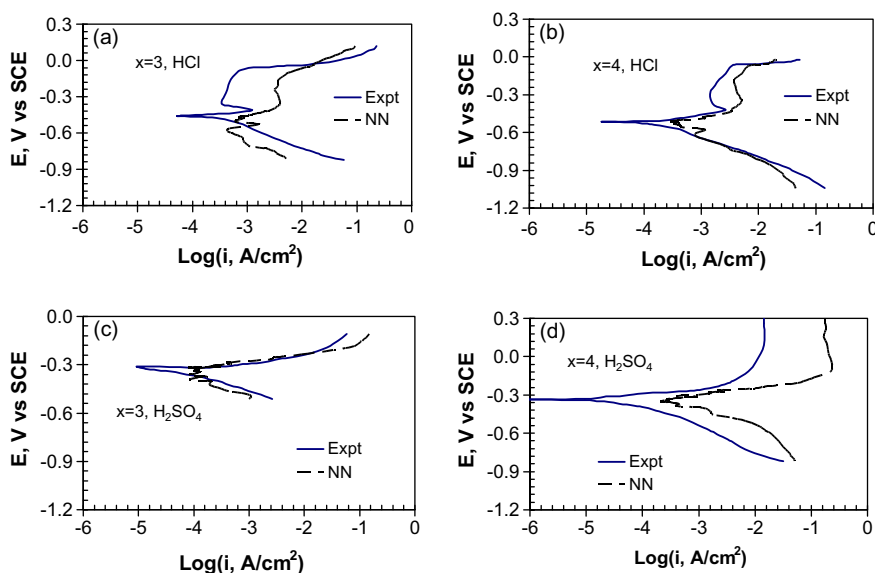

Fig. 5. Experimental and NN predicted polarization curves for $Fe_{68}Ni_{14-x}Mo_xSi_2B_{16}$ metallic glasses with (a) $x = 3$ in 1 M HCl, (b) $x = 4$ in 1 M HCl, (c) $x = 3$ in 0.5 M H_2SO_4, and (d) $x = 4$ in 0.5 M H_2SO_4. The NN prediction used data sets that were not seen by the model during training.

satisfactory. Moreover, it was noted by the authors of the source article that the experimental polarization curves for metallic glasses in HCl did not appear to be systematic with the changes in the material compositions. Also, as was shown in the same article, the same kinetic parameters for metallic glasses in HCl calculated from impedance data were significantly different than the ones obtained from the polarization curves. Therefore, it appears that the differences in the model prediction with the test data sets not seen by the model during training can possibly be due to some problems in the samples or some other possible reasons not explained in the source article. Corrosion potentials and polarization resistances that are direct measures of corrosion behavior were calculated from the polarization and are presented in Table 3a along with the same parameters calculated from the experimental polarization curves. Goodness of fit were measured using a metric R^2 (Square of the Pearson Product-Moment Correlation Coefficient) and the results are shown in Table 3b. As is observed, both validation and test data resulted in high correlation between estimation/prediction and experimental values. R^2 values ranged from 0.92 to 0.97 for HCl and 0.82 to 0.98 for H_2SO_4 with an exception in the HCl medium for $x = 3$ for which calculated R^2 value was 0.56. However, the reason for this has been explained earlier. Results in the figures and tables show that the model could, mostly, well predict the corrosion potentials and polarization resistances for the alloy under study.

4.2. General corrosion, DC data on carbon and alloy steel using weight losses [4,5]

Another type of information collected is shown in Table 4. Carbon and alloy steel are widely used alloys and as such, there have been numerous studies on the corrosion behavior of these alloys – a few among them are described in Refs. [23–27]. The data collected on carbon and alloy steel by several authors included the environment, type of metal alloy (composition), temperature, and metal dissolution rate under the specified condition and at a given time.

Carbon and alloy steel data were analyzed at different environmental conditions (including temperature, pH and other varied conditions). Mediums of corrosion were numbered as: hydrofluoric acid-1, sulfuric acid-2, phosphoric acid-3, chlorosulfonic acid-4, sodium hydroxide-5, atmospheric environments-6, calcium bromide-7, ammonium sulfite-8, sodium hypochlorite-9, potassium hydroxide-10, and seawater-11. Data were organized according to the differences in the conditions (combination of environmental properties) and environmental conditions were numbered from 1 to 6. Each condition was uniquely different from the others. However, a common basis was not present in the data so that they could be separated as individual input variable or parameter. Data were used for model development by considering the conditions simultaneously as well as separately. We developed a model in which the environment, metal description and metal compositions were labeled, and the information was used to map the environ-

ments and material composition to general corrosion rate by means of a supervised neural network (NN). As in the case of metallic glasses, a hyperbolic tangent (tanh) function was used as the transfer function in the ANN model, the Levenberg–Marquardt algorithm was used as the optimization algorithm, and the error minimization tolerance was set to 1%. The topology of the ANN for each of the six conditions was as follows: 15 inputs, three hidden layers consisting of 50, 50, and 20 neurons, respectively, and 2 outputs. The inputs were: compositions (of B, C, Cr, Cu, Fe, Mn, Mo, Ni, P, S, Si, Ti, and V), duration of exposure, and log(duration of exposure). The outputs were: corrosion rate and log(corrosion rate). The ANN model was trained for short time period and the corrosion rate was predicted with test data set for longer time period. The NN model was able to predict long term corrosion rate that was in very good agreement with the experimental data. Fig. 6(a)–

Table 3b
Goodness of fit, R^2 (Square of the Pearson Product-Moment Correlation Coefficient) for the neural network estimation and prediction. Validation and test data sets on $Fe_{68}Ni_{14-x}Mo_xSi_2B_{16}$ metallic glasses in 1 M HCl and 0.5 M H_2SO_4 were used in comparison to the experimental data.

Samples	R^2 Value: Expt. vs NN		Avg. R^2 Value	
	1 M HCl	0.5 M H_2SO_4	1 M HCl	0.5 M H_2SO_4
$x = 0$	0.97	0.98	0.87	0.89
$x = 1$	0.92	0.88		
$x = 2$	0.96	0.90		
$x = 3$	0.56	0.82		
$x = 4$	0.95	0.90		
E_{corr}	1	1		
R_p	1	1		

Table 4
Sample of corrosion rate data on carbon and alloy steel received from NIST in different environments [4,5].

Environ	Material	Rate, mm/yr	Rate, mpy	UNS	Temperature, °C	Duration
Atmospheric	Carbon steel	0.055	2.2	G10100	25	.25–4 yr
Atmospheric	Carbon steel	0.026	1.04	G10100	25	.25–4 yr
Atmospheric	Carbon steel	0.027	1.08	G10100	25	.25–4 yr
NaCl	4340 steel	0.55	21.8	G43400	25	
NaCl	4130 steel	0.09	3.5	G41300	150	30 days
NaCl	4130 steel	0.29	11.7	G41300	200	30 days
HCl	1020 steel	2.1	83	G10200	500	15 days
HCl	1020 steel	0.3	13	G10200	400	15 days
HCl	1020 steel	0.7	28	G10200	300	15 days

Table 3a
Neural network estimated corrosion potential and polarization resistance for $Fe_{68}Ni_{14-x}Mo_xSi_2B_{16}$ metallic glasses in 1 M HCl and 0.5 M H_2SO_4, in comparison to the same parameters calculated from experimental polarization data. Note that test data sets for $x = 3$, 4 in 1 M HCl and $x = 4$ in 0.5 M H_2SO_4 have not been used in modeling (boldface results).

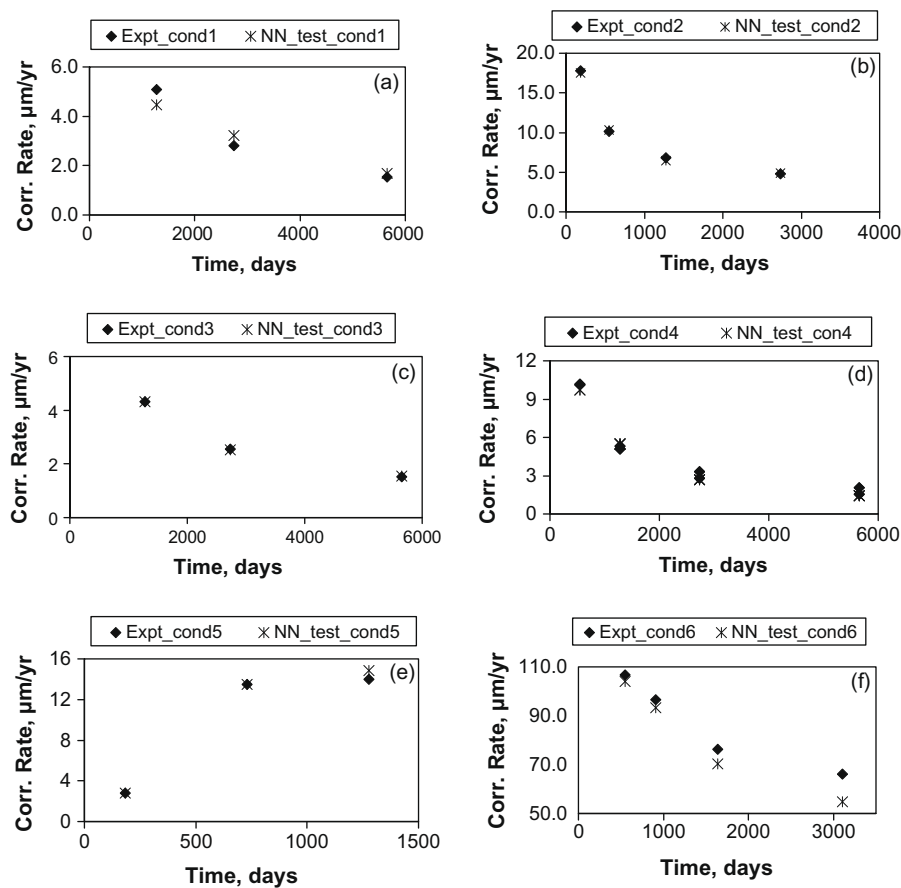| Samples	1 M HCl				0.5 M H_2SO_4			
	Polarization Expt		Neural network (NN)		Polarization Expt		Neural network (NN)	
	E_{corr}, mV vs SCE	R_p, ohm cm^2	E_{corr}, mV vs SCE	R_p, ohm cm^2	E_{corr}, mV vs SCE	R_p, ohm cm^2	E_{corr}, mV vs SCE	R_p, ohm cm^2
$x = 0$	−571	201	−565	202	−357	2774	−310	2695
$x = 1$	−540	103	−525	112	−290	154	−300	153
$x = 2$	−567	167	−560	165	−310	148	−290	148
$x = 3$	−506	41	**−550**	**135**	−317	264	−325	225
$x = 4$	−554	142	**−533**	**97**	−331	116	**−310**	**92**

Fig. 6. Experimental and NN predicted corrosion rates for carbon and alloy steel at environmental conditions: (a) Condition 1, (b) Condition 2, (c) Condition 3, (d) Condition 4, (e) Condition 5, and (f) Condition 6. Expt_condNo.: experimental data. NN_ind_test: corrosion rate was predicted using test data sets that were not seen by the neural network model during the training.

(f) and Table 5 show the comparison of corrosion rates from experimental observations and NN predictions for carbon and alloy steel in six different environmental conditions. R^2 (Square of the Pearson Product-Moment Correlation Coefficient) values were used as a measure of goodness of fit for validation and test data sets and the results are shown in Table 5. It is observed that the test data resulted in high correlation between estimation/prediction and experimental values. R^2 values ranged from 0.95 to 0.99 with an average value of 0.987.

5. Database mining of localized corrosion data on metal alloys

5.1. Localized corrosion: crevice corrosion on Ti-alloy [6]

Localized corrosion such as pitting and crevice corrosion is one of the most damaging corrosion types for metals and alloys. As such, there has been tremendous interest in studying localized corrosion. Theoretical deterministic methods are typically developed to predict localized corrosion damage [28–38]. Before using the model, experimental data is used to find deterministic-model related parameters that are unknown. The model uses measured DC and AC impedance data which are fitted to the predicted DC and AC curves to extract those unknown model parameters; and then the model is used to predict corrosion damage under different environmental scenarios. The model parameters are specific to an alloy composition. Accordingly, to predict the corrosion damage for other alloy composition, it would be necessary to collect DC and AC data and fit those unknown model parameters to the

new data. An example of such parameters is given in Table 6. Localized corrosion of Ti-based alloys has been studied by several researchers [39–42]. We here used the data collected by He et al. [6] who developed a damage function of the form $D_{max} = kt^n$ where D_{max} is the maximum penetration depth (typically in micrometer (µm)), t is time (typically in days), and k and n are unknown parameters. The values of the parameters are calculated using experimental data and the units of the parameters depend on the units of penetration depth and time. The parameter values for k and n were found to be 89.74 and 0.9897, respectively, for crevice corrosion of Ti-2 in a 0.27 mol/dm^3 NaCl solution at 95 °C, where units of penetration depth and time were µm and days, respectively [6]. Other measured parameters in the study were: weight change (W) which was used to determine the total extent of corrosion, extent of corrosion due to the external O_2 reduction on the counter electrode (Q), and percentage of O_2 consumed during the process which is directly related to the corrosion damage caused by O_2 reduction. Q was determined by integrating the crevice current and was expressed in the units of charge. The percentage of O_2 consumed was calculated from the initial amount of O_2 and the O_2 consumed during the experiment ($Q/4F$, F being Faraday's constant). The ratio Q/W (the units of W is converted to the units of charge by using Faraday's law) represents the extent of corrosion driven by the external O_2 reduction.

The use of the mapping data to signatures (AC or DC) does not require a model. Therefore, we may not want to mimic the model but "short-cut" the model, and then, create a model that can make predictions of the localized damage. Then, use the existing model to compare and contrast the predictions.

Table 5
Experimental and NN predicted corrosion rates for alloy steel at different environmental conditions.

Alloy type	UNS	Environmental condition	Duration of exposure, days	Data type	Corr. rate, μm/yr	R^2 Value: Expt vs NN	Avg. R^2 Value
Carbon and alloy steel	K11630	1	1277.5	Expt	5.08	0.952	0.987
				NN	4.48		
			2737.5	Expt	2.79		
				NN	3.22		
			5657.5	Expt	1.52		
				NN	1.69		
		2	182.5	Expt	17.78	0.998	
				NN	17.51		
			547.5	Expt	10.16		
				NN	10.31		
			1277.5	Expt	6.86		
				NN	6.48		
			2737.5	Expt	4.83		
				NN	4.90		
		3	1277.5	Expt	4.32	0.999	
				NN	4.31		
			2737.5	Expt	2.54		
				NN	2.54		
			5657.5	Expt	1.52		
				NN	1.53		
		4	547.5	Expt	10.16	0.983	
				NN	9.65		
			1277.5	Expt	5.08		
				NN	5.59		
			2737.5	Expt	2.79		
				NN	2.70		
			5657.5	Expt	1.52		
				NN	1.42		
		5	182.5	Expt	2.79	0.996	
				NN	2.79		
			730	Expt	13.46		
				NN	13.46		
			1277.5	Expt	13.97		
				NN	14.87		
		6	3102.5	Expt	66.04	0.995	
				NN	54.71		
			1642.5	Expt	76.20		
				NN	70.37		
			912.5	Expt	96.52		
				NN	93.34		
			547.5	Expt	106.68		
				NN	103.90		

Table 6a
Data used to develop a damage function for crevice corrosion of Ti-2 in a 0.27 mol/dm^3 NaCl solution at 95 °C, where Q and W represent electronic charge difference and weight change, respectively.

Incubation period, days	Duration, days	Maximum penetration depth, D_{max}, mm	Q, C	Weight change, g	Q/W	O_2 consumed, %
1.19	3.02	140	9.03	0.0525	0.0143	0.5
2.42	9.78	604	106	0.0773	0.114	5
0.54	15.13	938	371	0.1595	0.193	19
0.76	15.5	969	333	0.2728	0.101	17
1.31	23.15	1265	578	0.2333	0.206	29
1.22	31.07	1645	899	0.321	0.232	45

Table 6b
Goodness of fit, R^2 (Square of the Pearson Product-Moment Correlation Coefficient) for the neural network estimation. Validation data (estimated and experimental) on Ti-2 in a 0.27 mol/dm^3 NaCl solution at 95 °C were used for comparison.

R^2 Value: Expt. vs NN			
Max. penetration depth, D_{max}	Weight change, W	Q	O_2 consumed
1	1	1	1

Data on the effect of incubation period and the duration of experiments on maximum pit depth, the effect of duration of experiment on the weight change due to corrosion and the effect of duration of experiment on total O_2 consumption during the experiment were used for the model development and validation. As before, a hyperbolic tangent (tanh) function was used as the transfer function in the ANN model, the Levenberg–Marquardt algorithm was used as the optimization algorithm, and the error minimization tolerance was set to 1%. The topology of the ANN was as follows: 2 inputs, three hidden layers consisting of 20, 20, and 20 neurons, respectively, and 10 outputs. The inputs were: incubation period and the duration of experiments. The outputs were: maximum pit depth D_{max}, sample weight change W, charge amount Q, ratio Q/W, O_2 consumed, $\log(D_{max})$, $\log(W)$, $\log(Q)$, $\log(Q/W)$, and $\log(O_2$ consumed). There were eight samples for training and validation of the ANN model. Prediction of maximum pit depth, sample weight change, and O_2 consumption was conducted using user-specified duration of time and were compared with the experimental data available for the same period of time. Results are shown in Fig. 7(a)–(e). The NN model shows very good agreement with the portion of data available from the experiment. Again, R^2 values were used as a measure of goodness of fit and the results shown in Table 6b) indicate 100% correlation. Note that due to the small number of experimental data points available, it was not practical to divide the data set into training and test sets. Validation data (estimated and experimental) on Ti-2 in a 0.27 mol/dm^3 NaCl solution at 95 °C were used for comparison. If we compare the maximum pit depth prediction using the empirical model developed by He et al. [6] and the NN model developed in this
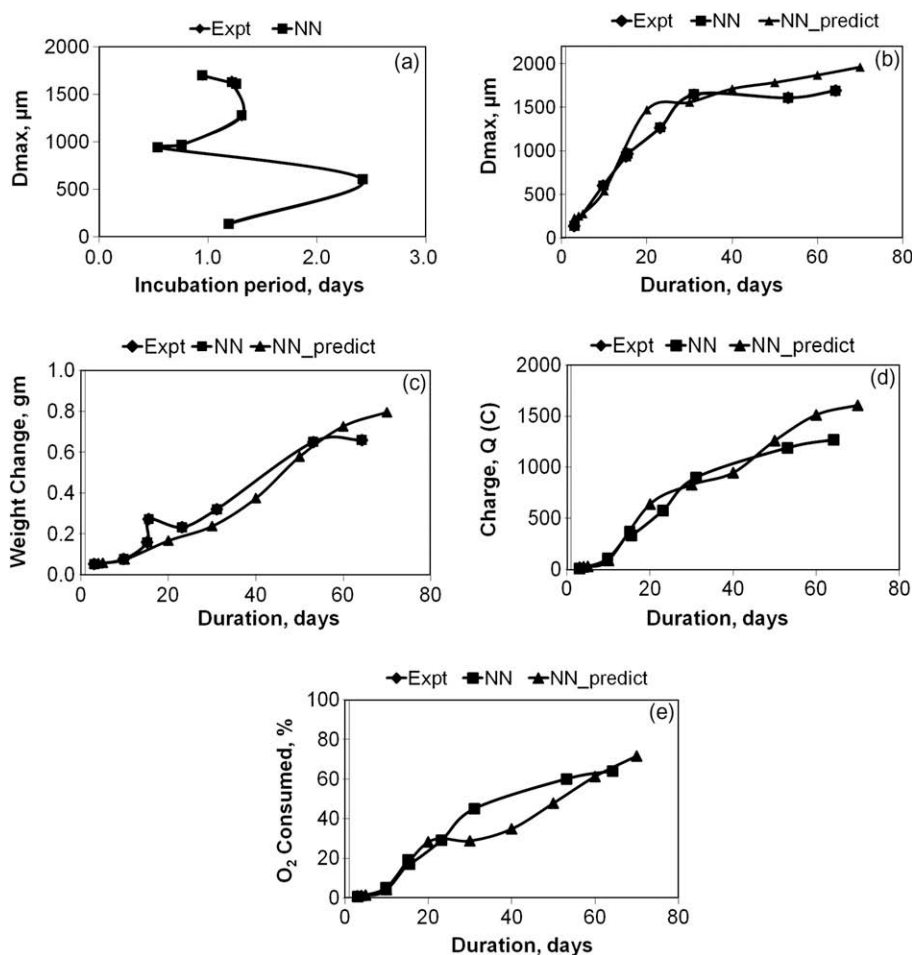
Fig. 7. Experimental data and NN model predicted results in the study of crevice corrosion of grade-2 titanium in 0.27 mol/dm^3 NaCl solution at 95 °C. (a) Influence of incubation period on maximum pit depth, D_{max}, (b) prediction of maximum pit depth, D_{max}, (c) prediction of sample weight change, (d) prediction of O_2 consumption, and (e) prediction of electronic charge difference, Q. Expt: experimental data, NN: model prediction using the same input data that was used for training, NN_predict: neural network prediction for 7.0 years with test data not seen by the model.

paper, the results are in very good agreement. Moreover, the NN model is more flexible and is able to capture complex system behavior that sometimes may not be possible when using a deterministic approach that requires the specification of mathematical expressions or the physics of the system dynamics.

6. Summary and conclusions

A supervised neural network (NN) mapping using 'backpropagation' method was developed for metal alloys such that the NN model learns the underlying functions in mapping corrosion variables and parameters to different corrosion metrics (corrosion rate, corrosion potential, crevice repassivation potential, etc.).

Corrosion data on corrosion allowable (e.g. Fe-alloy, carbon and alloy steel) as well as corrosion resistive (e.g. Ti) alloys were collected from mainly publicly available articles and personal communication. Both general corrosion data and localized corrosion data were collected, pre-processed (transformed, cleansed, integrated, and normalized), and used in the NN analysis.

NN model developed using polarization data for general corrosion of metallic glasses show good agreement with experimental data at the specified operating condition when the model prediction was validated using test data (experimental) sets. Validation of the developed NN model using carbon and alloy steel data from the NIST show very good agreement between experimental and predicted corrosion rates when the model was developed using data under individual environmental conditions. The NN model developed using crevice corrosion data on grade-2 titanium was validated against experimental data to show excellent agreement. The model was then used to predict future maximum pit depth and other variables of interest under similar operating conditions. R^2 values, a measure of goodness of fit of test data show very good agreements between estimation/prediction and experiments.

References

[1] J. Han, M. Kamber, Data Mining: Concepts and Techniques, Morgan Kaufman, San Francisco, USA, 2001.
[2] M.J.A. Berry, G.S. Linoff, Mastering Data Mining: The Art and Science of Customer Relationship Management, second ed., John Wiley and Sons Inc., 2000.
[3] B. Seshu, A.K. Bhatnagar, A. Venugopal, V.S. Raja, J. Mater. Sci. 32 (1997) 2071.
[4] J.D. Trim, D.B. Anderson, G.J. Laverty, The NACE–NBS Corrosion Data Program, in: 10th International Congress on Metallic Corrosion, Madras, India, vol. II, 1987, Key Eng. Mater. 20–28 (1988) 1781.

[5] C.P. Sturrock, W.F. Bogaerts, Classification and prediction of the corrosion behavior of nickel-containing alloys from field test data, in: ASTM STP 1311, Computerization and Networking of Materials Databases, Tsukuba, Japan, vol. 5, 6–8 November, 1995, p. 144, 1997 ASTM, 100 Barr Harbor Drive, West Conshohocken, PA 19428-2959, USA.

[6] X. He, J.J. Nöel, D.W. Shoesmith, Corros. Sci. 47 (2005) 1177.

[7] C.M. Bishop, Neural Networks for Pattern Recognition, Oxford University Press, Oxford, 1995.

[8] B.D. Ripley, Pattern Recognition and Neural Networks, Cambridge University Press, 1996.

[9] H.K.D.H. Bhadeshia, Neural Networks in Materials Science, ISIJ Int. 39 (1999) 966.

[10] A Great Practical Tutorial on Neural Networks. Available from: <http://www.ai-junkie.com/ann/evolved/nnt1.html>.

[11] R. Rojas, Neural Networks, Springer-Verlag, Berlin, 1996.

[12] E. Angelini, C. Antonione, M. Baricco, F. Bianco, F. Rosalbino, F. Zucchi, Werkst. Korros. (1993) 98.

[13] H. Choi-Kim, D. Xu, W.L. Johnson, J. Metastable Nanocryst. Mater. 20–21 (2004) 29.

[14] K. Asami, S.J. Pang, T. Zhang, A. Inoue, J. Electrochem. Soc. 149 (2002) B366.

[15] S. Pang, T. Zhang, K. Asami, A. Inoue, Mater. Trans. 43 (2002) 2137.

[16] C. Qin, W. Zhang, H. Nakata, H. Kimura, K. Asami, A. Inoue, Mater. Trans. 46 (2005) 858.

[17] K. Mohri, IEEE Trans. Mag. MAG-20 (1984) 942.

[18] C.H. Smith, K. Nathasingh, in: J. Thompson (Ed.), Soft Magnetic Materials, University College, Cardiff, 1985.

[19] H. Warlimont, in: S. Steeb, H. Warlimont (Eds.), Proc. 5th Int. Conf. Rapidly Quenched Metals, Amsterdam, vol. 2, 1985, p. 1599.

[20] J.J. Croat, R.U. Herbst, R.W. Lee, et al., J. Appl. Phys. 55 (1984) 2078.

[21] L.A. Bailey, H. Lowdermilk, A.C. Lee, J. Magn. Mater. 54 (1986) 1618.

[22] NeuralWare Professional II/Plus, NeuralWare, 2005.

[23] D.N. Tsipas, G.K. Triantafyllidis, J. Kipkemoi Kiplagat, P. Psillaki, Mater. Lett. 37 (1998) 128.

[24] D. Starosvetsky, R. Armon, J. Yahalom, J. Starosvetsky, Int. Biodeterior. Biodegrad. 47 (2001) 79.

[25] L. Cáceres, T. Vargas, L. Herrera, Corros. Sci. 51 (2009) 971.

[26] Y.F. Cheng, J.L. Luo, Br. Corros. J. 35 (2000) 125.

[27] C.G. Peng, J.K. Park, Corrosion 50 (9) (1994) 669.

[28] D.D. Macdonald, M. Urquidi-Macdonald, Electrochim. Acta 31 (1986) 1079.

[29] M. Urquidi-Macdonald, D.D. Macdonald, J. Electrochem. Soc. 134 (1987) 41.

[30] D.D. Macdonald, M. Urquidi-Macdonald, J. Electrochem. Soc. 136 (1989) 961.

[31] T.R. Beck, R.C. Alkire, J. Electrochem. Soc. 126 (1979) 1662.

[32] F. Hunkeler, H. Böhni, Corrosion 37 (1981) 645.

[33] R.C. Alkire, K.P. Wong, Corros. Sci. 28 (1988) 411.

[34] G.S. Frankel, J. Electrochem. Soc. 145 (1998) 2186.

[35] B. Wu, J.R. Scully, J.L. Hudson, A.S. Mikhailov, J. Electrochem. Soc. 144 (1997) 1614.

[36] T.T. Lunt, S.T. Pride, J.R. Scully, J.L. Hudson, A.S. Mikhailov, J. Electrochem. Soc. 144 (1997) 1620.

[37] H.P. Hong, Corrosion 55 (1999) 10.

[38] G.S. Frankel, L. Stockert, F. Hunkeler, H. Böhni, Corrosion 43 (1987) 429.

[39] T.S. Rao, Aruna Jyothi Kora, B. Anupkumar, S.V. Narasimhan, R. Feser, Corros. Sci. 47 (2005) 1071.

[40] M.I. Abdulsalam, J. Mater. Eng. Perform. 16 (2007) 736.

[41] X. He, J.J. Noël, D.W. Shoesmith, J. Electrochem. Soc. 149 (2002) B440.

[42] X. He, J.J. Noël, D.W. Shoesmith, Corrosion 60 (2004) 378.

[43] Cooperative Agreement of Office of Science and Technology International of United States Department of Energy (DOE), the Office of Civilian Radioactive Waste Management (OCRWM), Office of Repository Development.